Electronic Supplementary Material (ESI) for RSC Advances.

Wide blue phase range observed in simple binary mixture systems containing rodlike racemic biphenyl mesogens with 2-octyloxy tail

Chiung-Cheng Huang,*[a] Chang-Yi Guo,[a] Wei-Cheng Hsieh,[a] Chih-Yi Fang,[a] Jian-Fu Chiou,[a] Mei-Ching Yu,[a] Bo-Hao Chen,[b] I-Jui Hsu*[b] and Jey-Jau Lee[c]

[a]*Department of Chemical Engineering, Tatung University, Taipei 104, Taiwan*

E-mail:chchhuang@ttu.edu.tw

[b]*Department of Molecular Science and Engineering, National Taipei University of Technology, Taipei 106, Taiwan*

E-mail: ijuihsu@ntut.edu.tw

Department of Chemical Engineering, Tatung University, Taipei 104, Taiwan.

[c]*National Synchrotron Radiation Research Center of Taiwan, Hsinchu 300, Taiwan*

Electronic supplementary information (ESI)

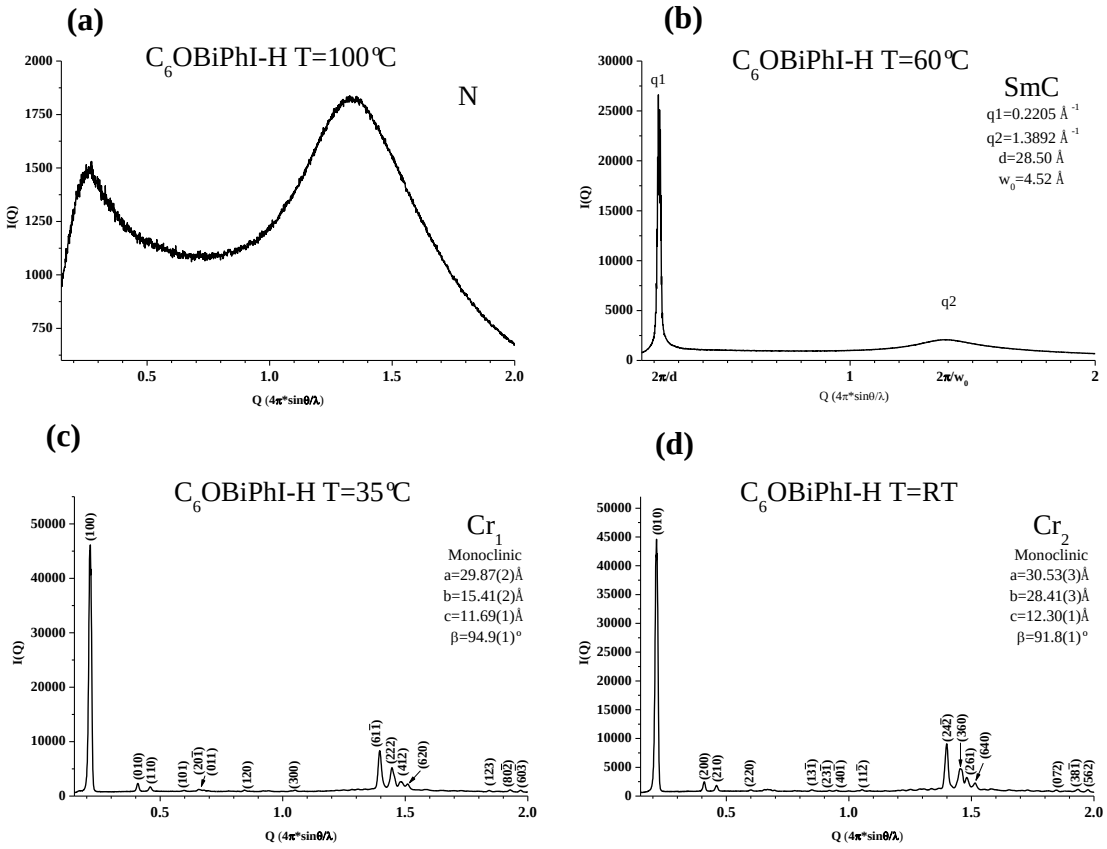

Fig. S1 The variable-temperature XRD measurements of biphenyl mesogen **C_6OBiPhI-H**

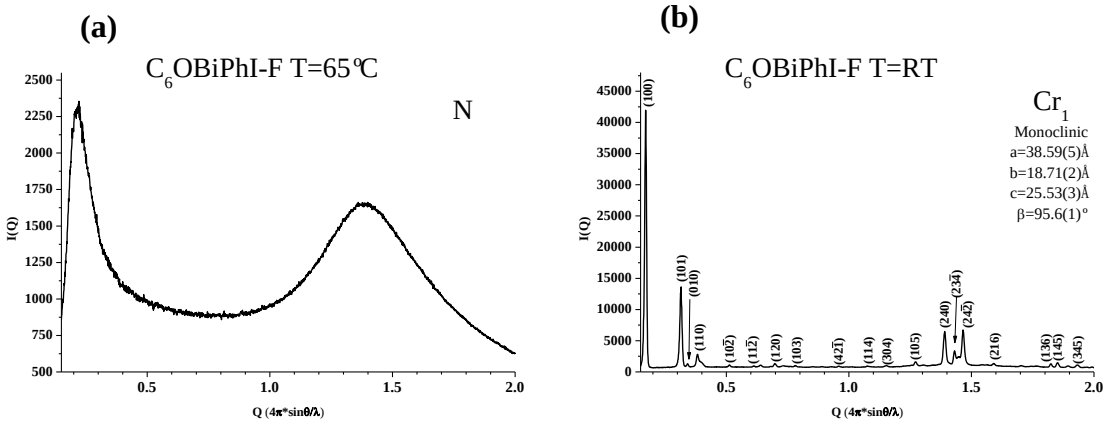

Fig. S2 The variable-temperature XRD measurements of biphenyl mesogen **C_6OBiPhI-F**

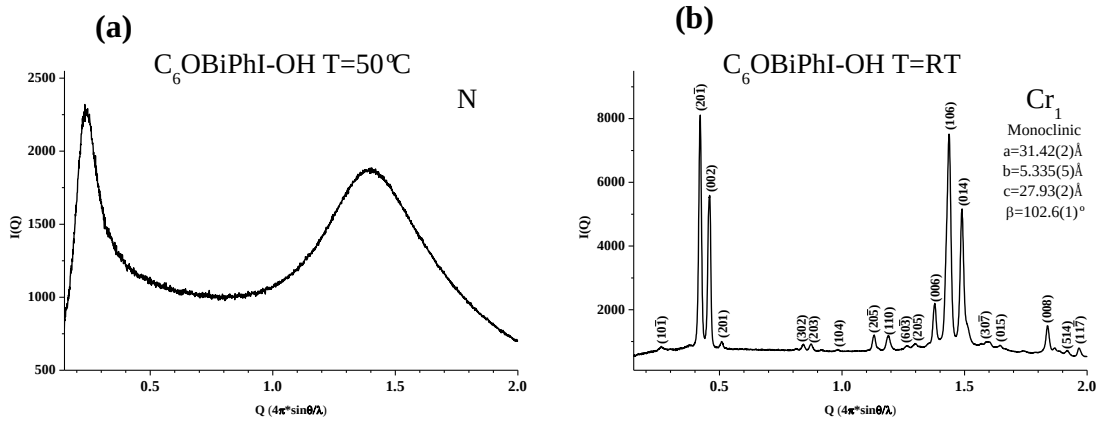

Fig. S3 The variable-temperature XRD measurements of biphenyl mesogen **C_6OBiPhI-OH**

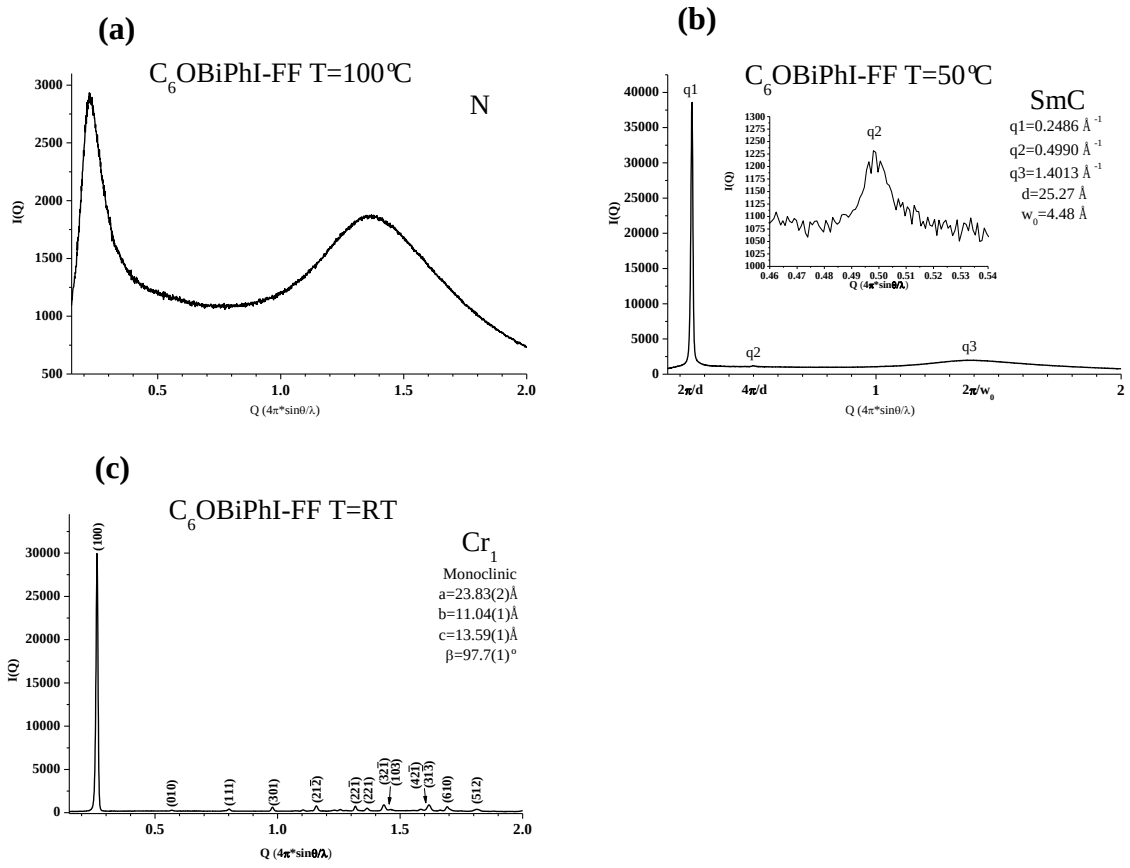

Fig. S4 The variable-temperature XRD measurements of biphenyl mesogen **C_6OBiPhI-FF**

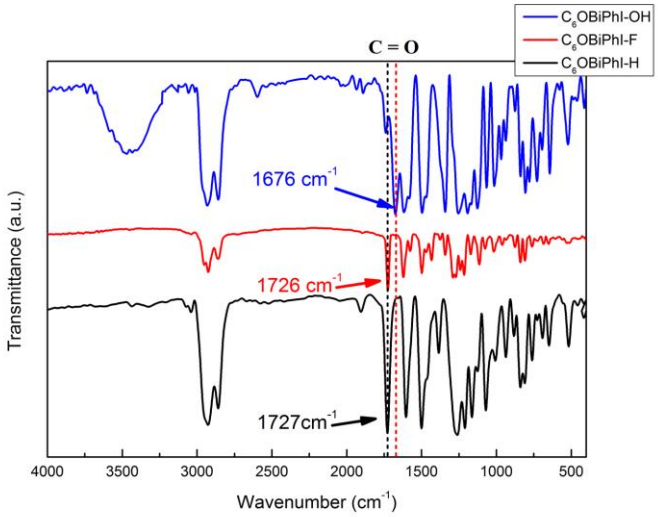

Fig. S5 FT-IR spectra of the biphenyl compounds **C_6OBiPhI-H**, **C_6OBiPhI-F** and **C_6OBiPhI-OH**.

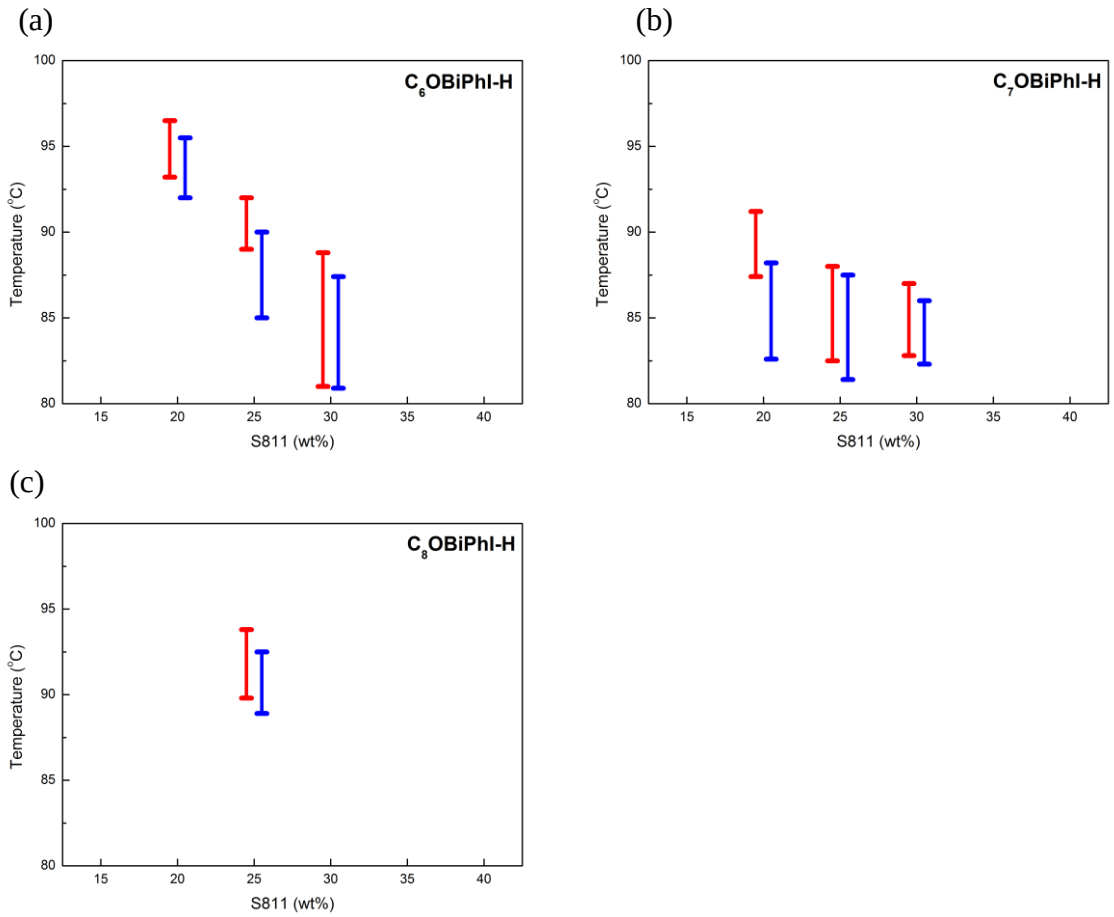

Fig. S6 The comparison of BP temperature range for the blending mixture system composed of **C_nOBiPhI-H** and different amount of chiral dopant **S811** in heating (red line) and cooling processes (blue line).

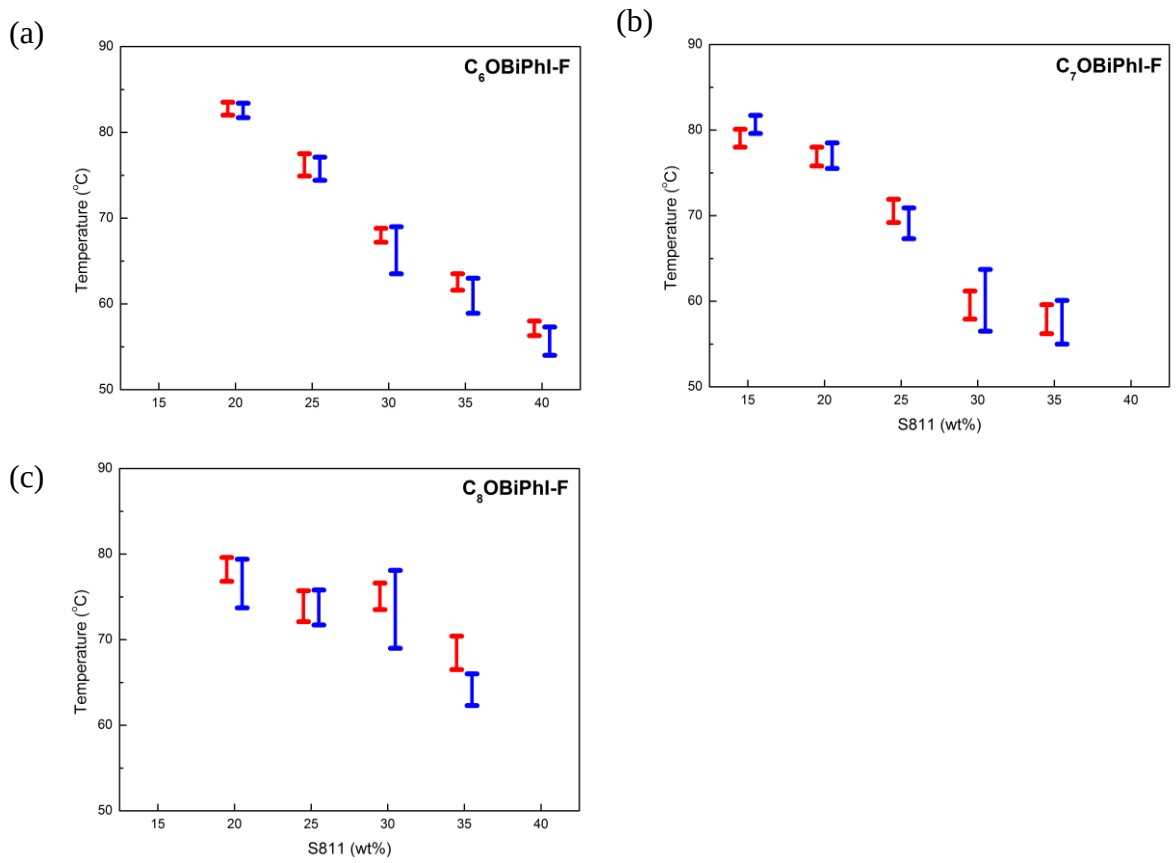

Fig. S7 The comparison of BP temperature range for the blending mixture system composed of **C_nOBiPhI-F** and different amount of chiral dopant **S811** in heating (red line) and cooling processes (blue line).

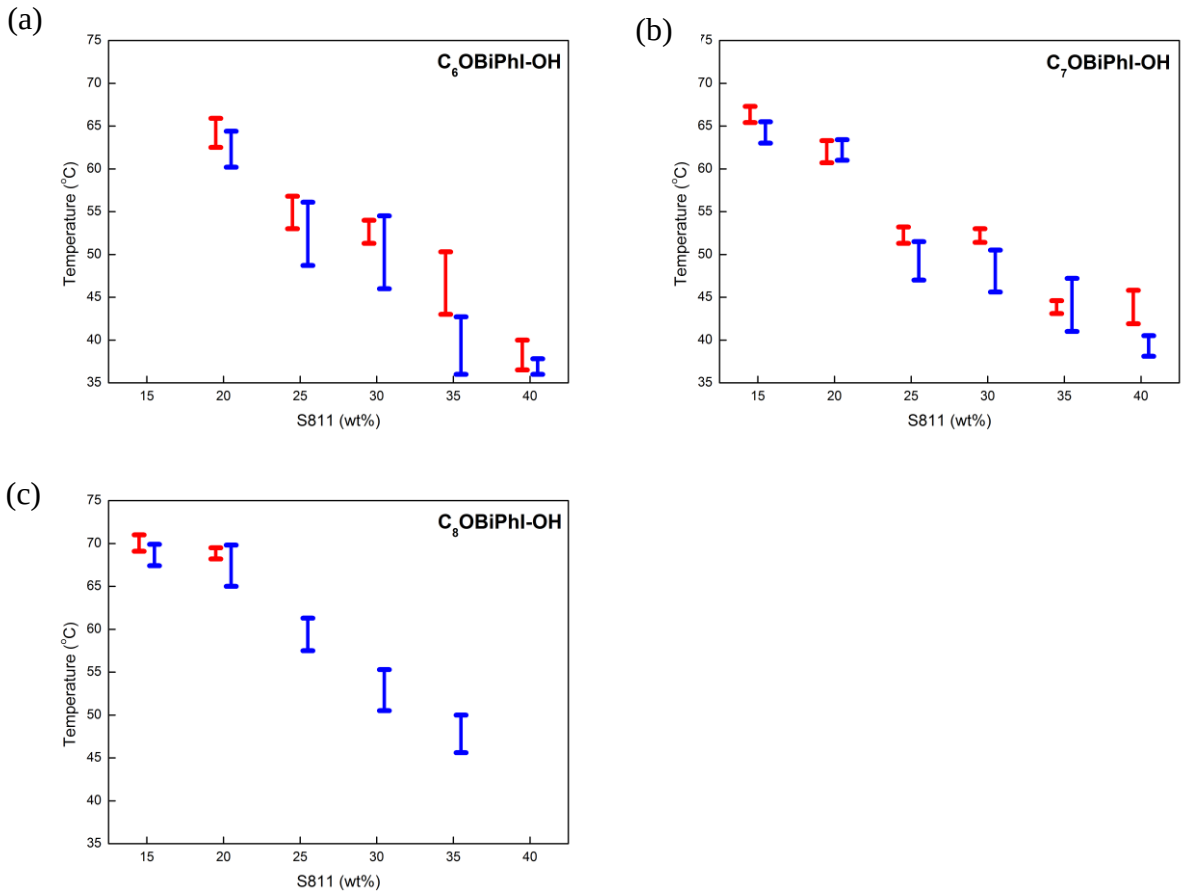

Fig. S8 The comparison of BP temperature range for the blending mixture system composed of **C_nOBiPhI-OH** and different amount of chiral dopant **S811** in heating (red line) and cooling processes (blue line).

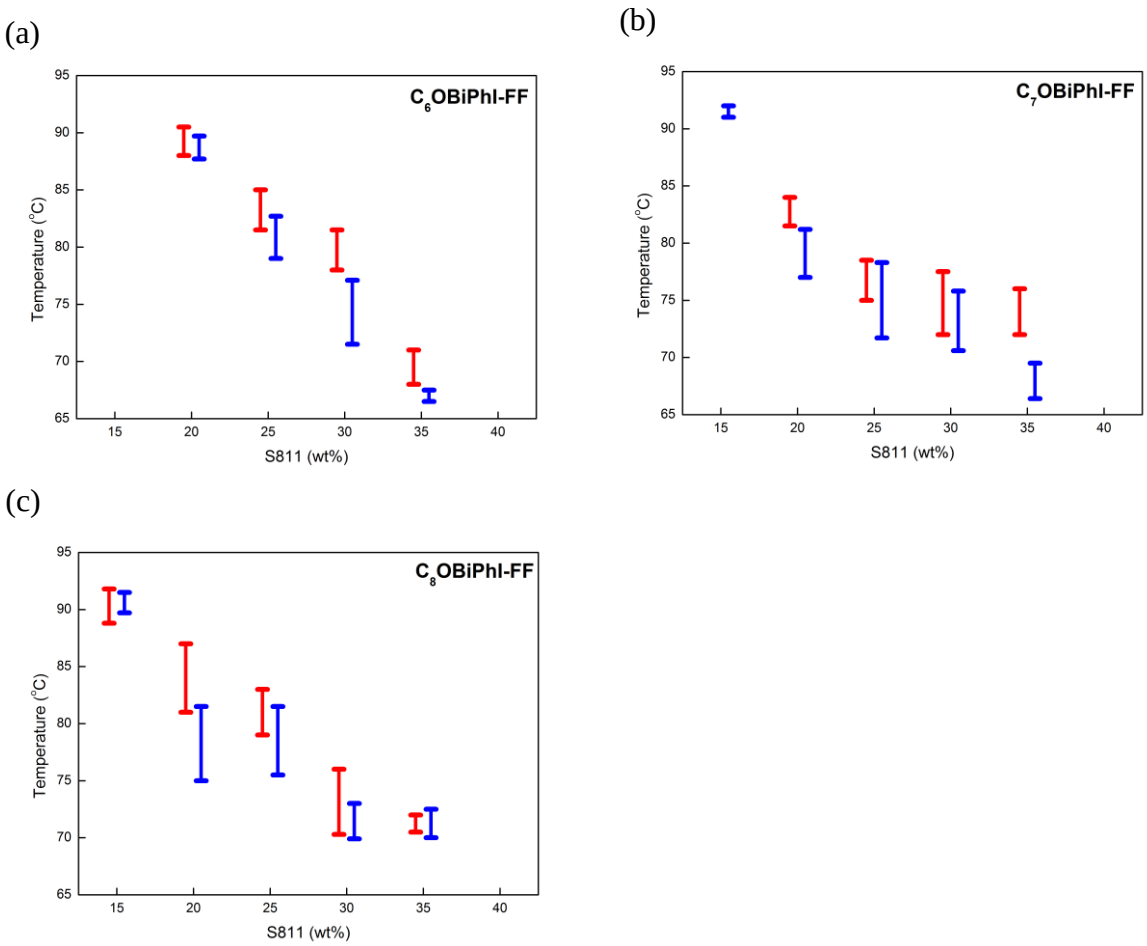

Fig. S9 The comparison of BP temperature range for the blending mixture system composed of **C_nOBiPhI-FF** and different amount of chiral dopant **S811** in heating (red line) and cooling processes (blue line).

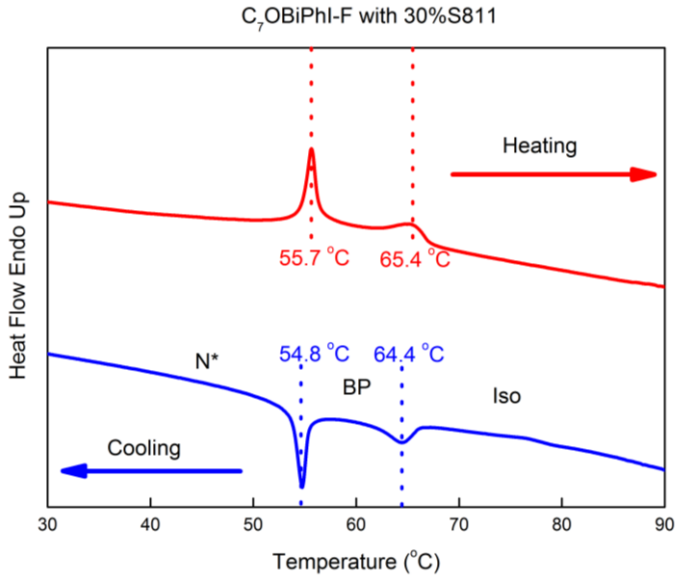

Fig. S10 DSC curves of **C_7OBiPhI-F** blended with 30.0 wt% **S811** (with rate of 1℃/min upon heating and cooling).

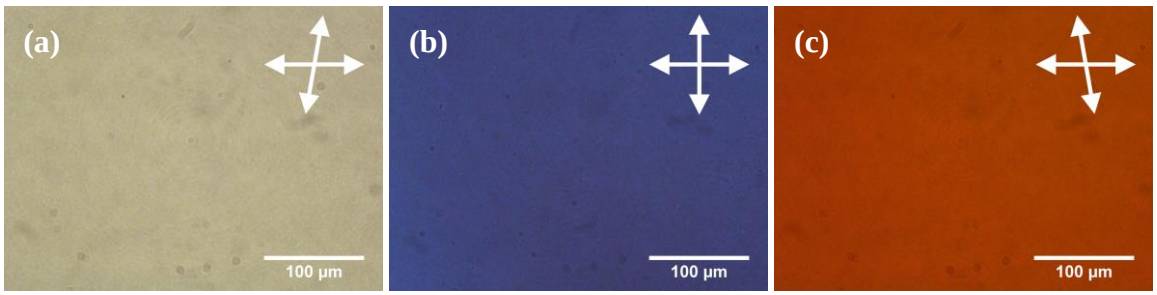

Fig. S11 Optical images of **C_7OBiPhI-OH** blended with 35.0 wt% **S811** were observed by POM at 46.0 °C (a) polarizer was rotated clockwise by a small angle of 10°. (b) Polarizer and analyzer were orthogonal. (c) Polarizer was rotated counterclockwise by a small angle of 10°.

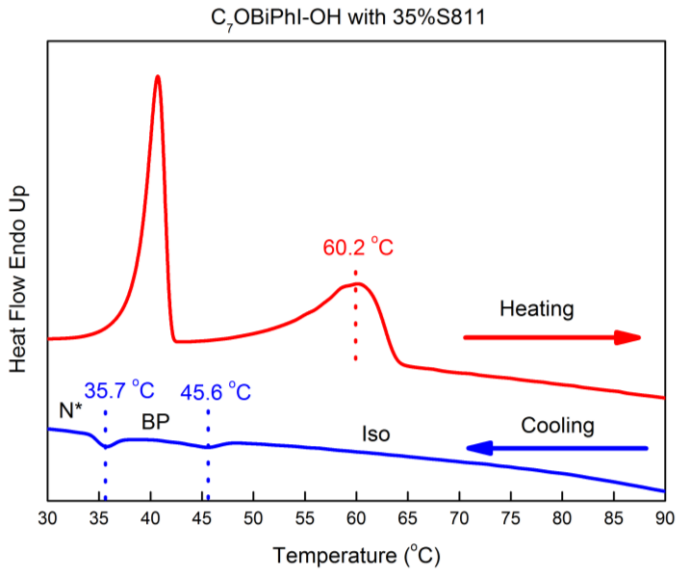

Fig. S12 DSC curves of **C_7OBiPhI-OH** blended with 35.0 wt% **S811** (with rate of 1℃/min upon heating and cooling).

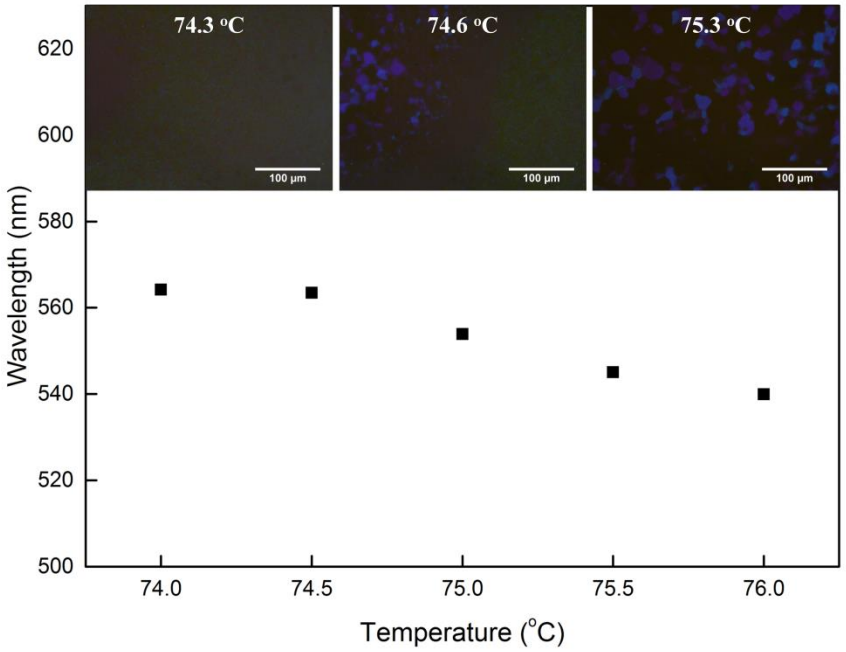

Fig. S13 The temperature dependence of the Bragg reflection wavelength for the blending mixture consisting of **C_8OBiPhI-F** + 30% **S811** during the heating process with a rate of 0.2 ℃ min^{-1}. The inset shows the POM images of BPs at different temperature.

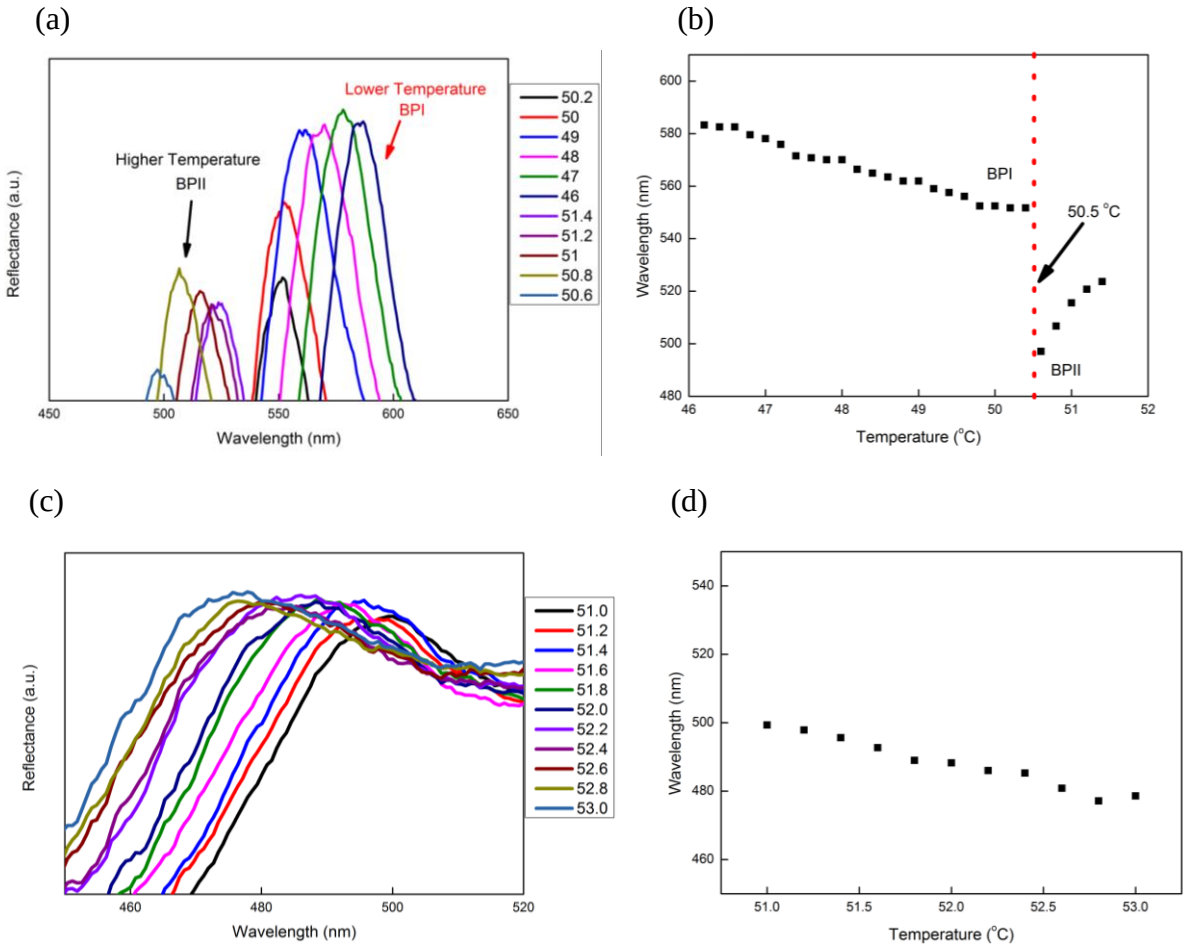

Fig. S14 For the blending mixture consisting of **C_7OBiPhI-OH** + 25% **S811** during the cooling process (a) Temperature dependence of typical reflectance profile, and during the heating process(c); (b) Temperature dependence of the Bragg reflection wavelength during the cooling process and, during the heating process (d) with a rate of 0.2 ℃ min^{-1}.

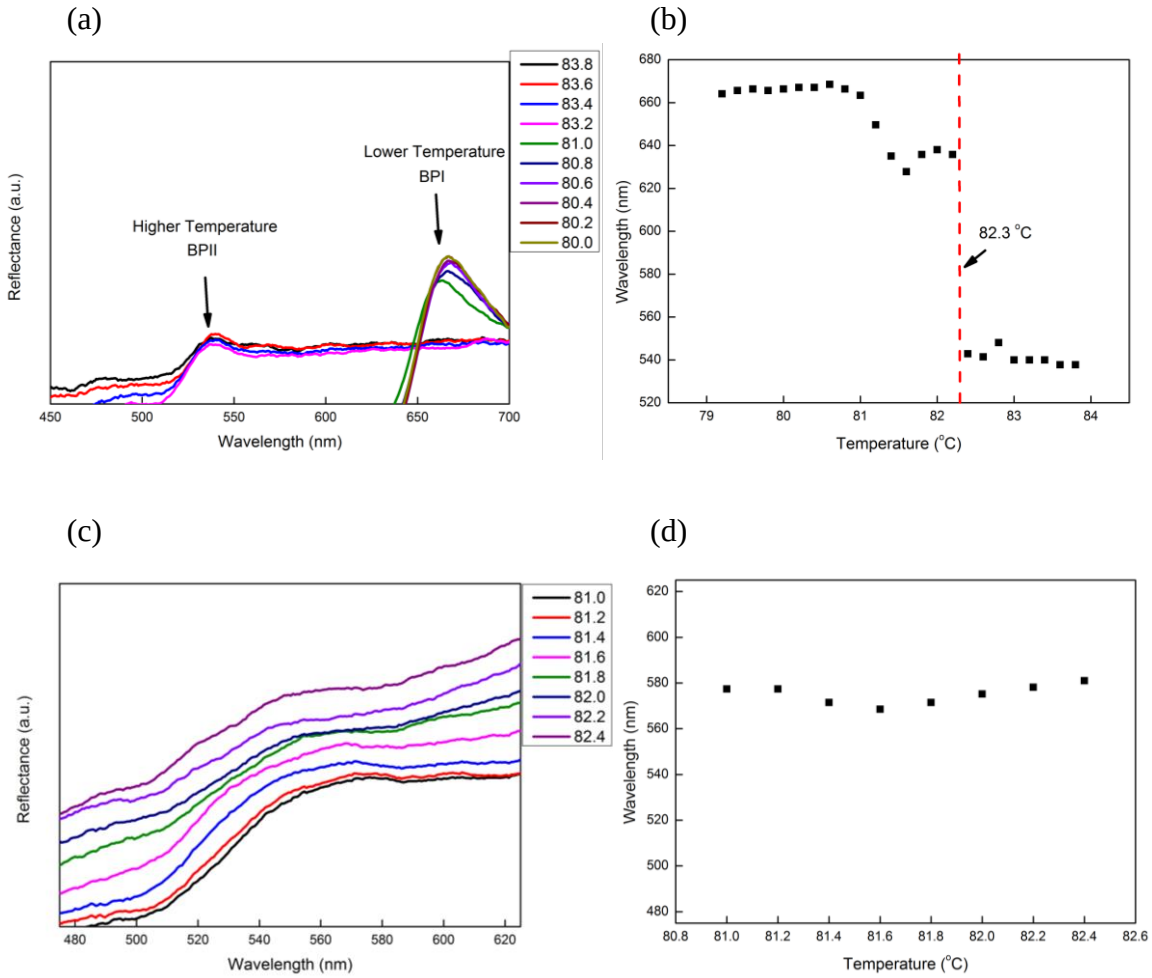

Fig. S15 (a) Temperature dependence of typical reflectance profile during the cooling process and (c) during the heating process; (b) Temperature dependence of the Bragg reflection wavelength during the cooling process and (d) during the heating process for the blending mixture consisting of **C_6OBiPhI-FF** + 25% **S811**. (with a rate of 0.2 °C min^{-1})

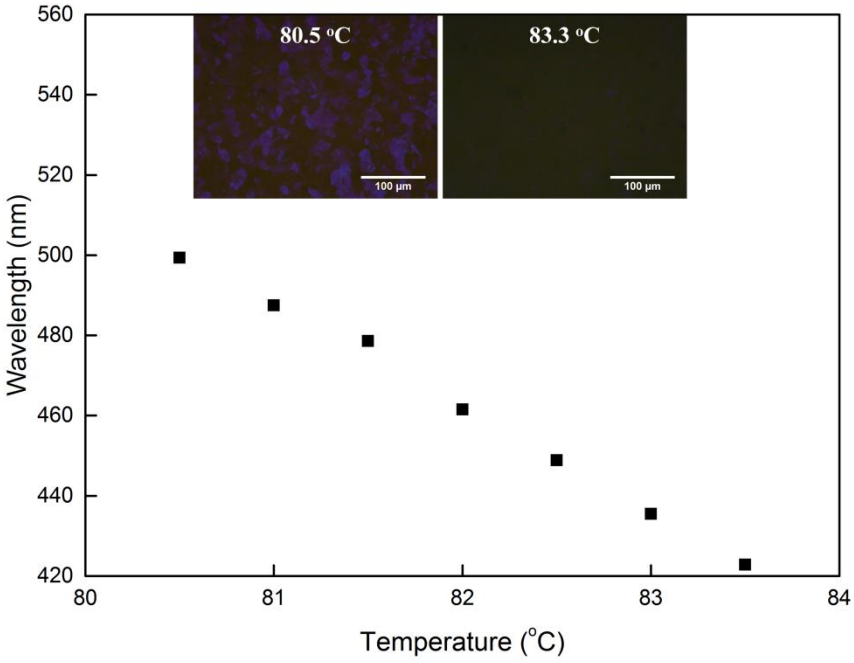

Fig. S16 The temperature dependence of the Bragg reflection wavelength for the blending mixture consisting of **C_8OBiPhI-F** + 10% **ISO(6OBA)$_2$** during the cooling process with a rate of 0.2 ℃ min^{-1}. The inset shows the POM images of BPs at different temperature.

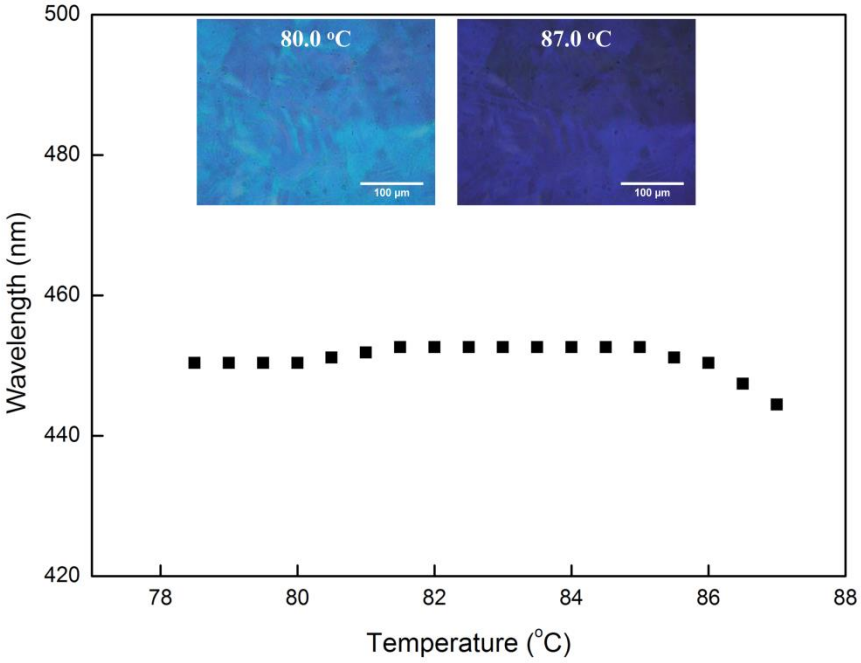

Fig. S17 The temperature dependence of the Bragg reflection wavelength for the blending mixture consisting of **C_8OBiPhI-FF** + 10% **ISO(6OBA)$_2$** during the cooling process with a rate of 0.2 ℃ min^{-1}. The inset shows the POM images of BPs at different temperature.

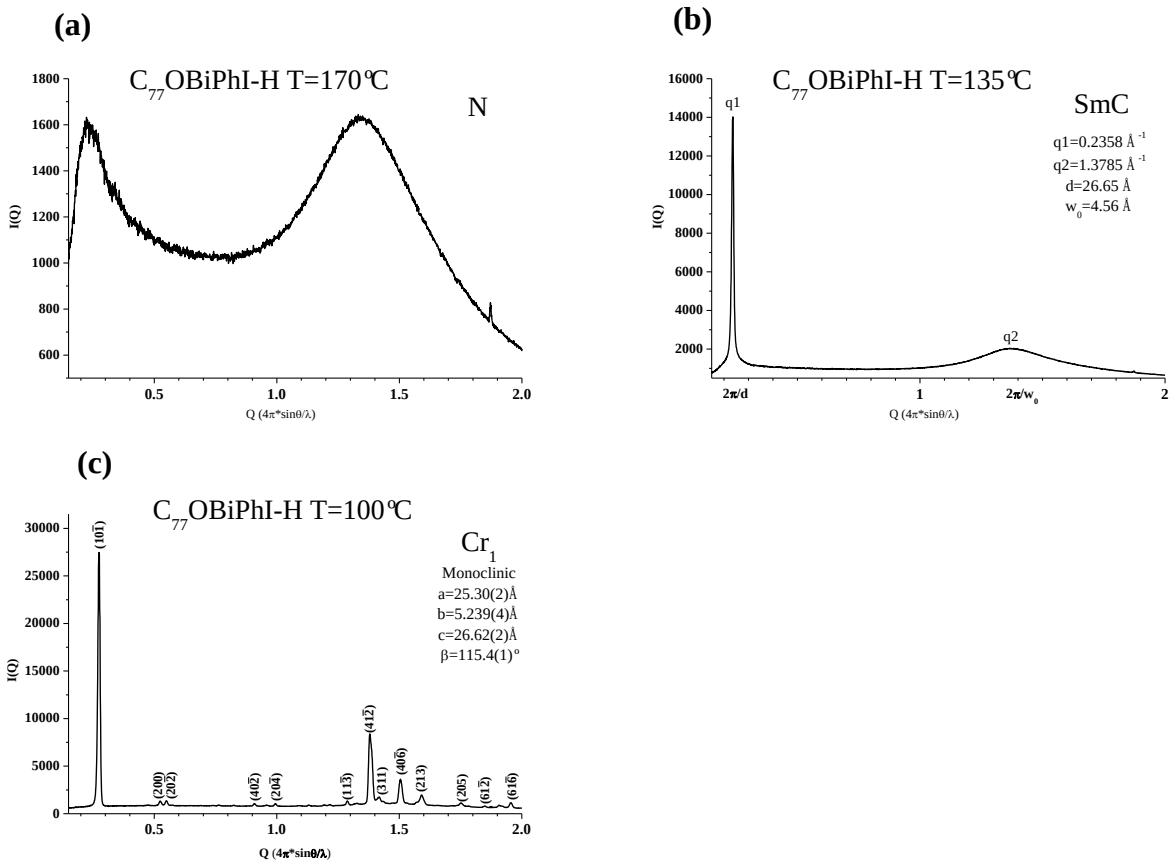

Fig. S18 The variable-temperature XRD measurements of biphenyl mesogen **C_6OBiPhI-FF**

(a)

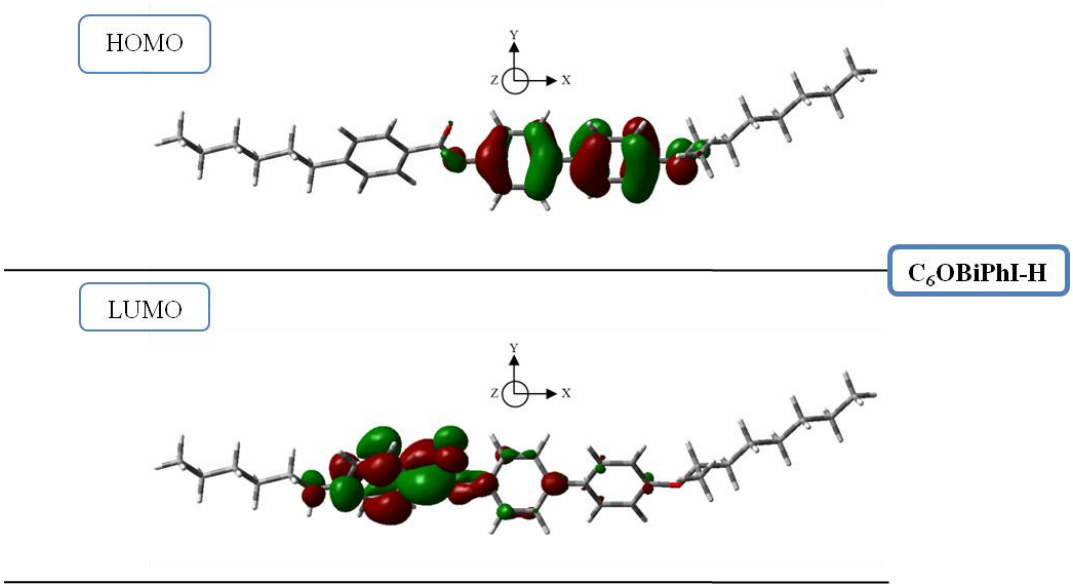

(b)

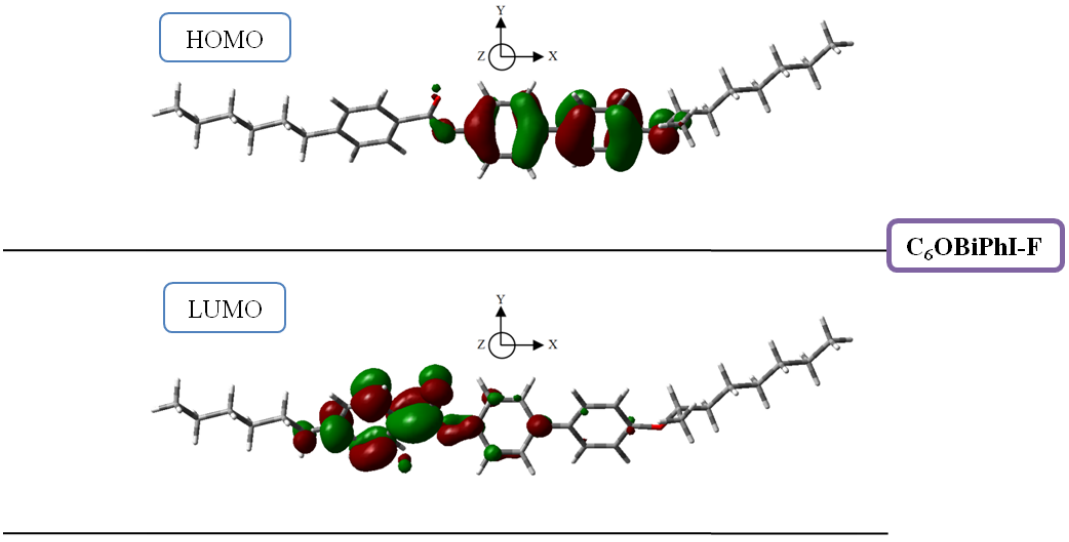

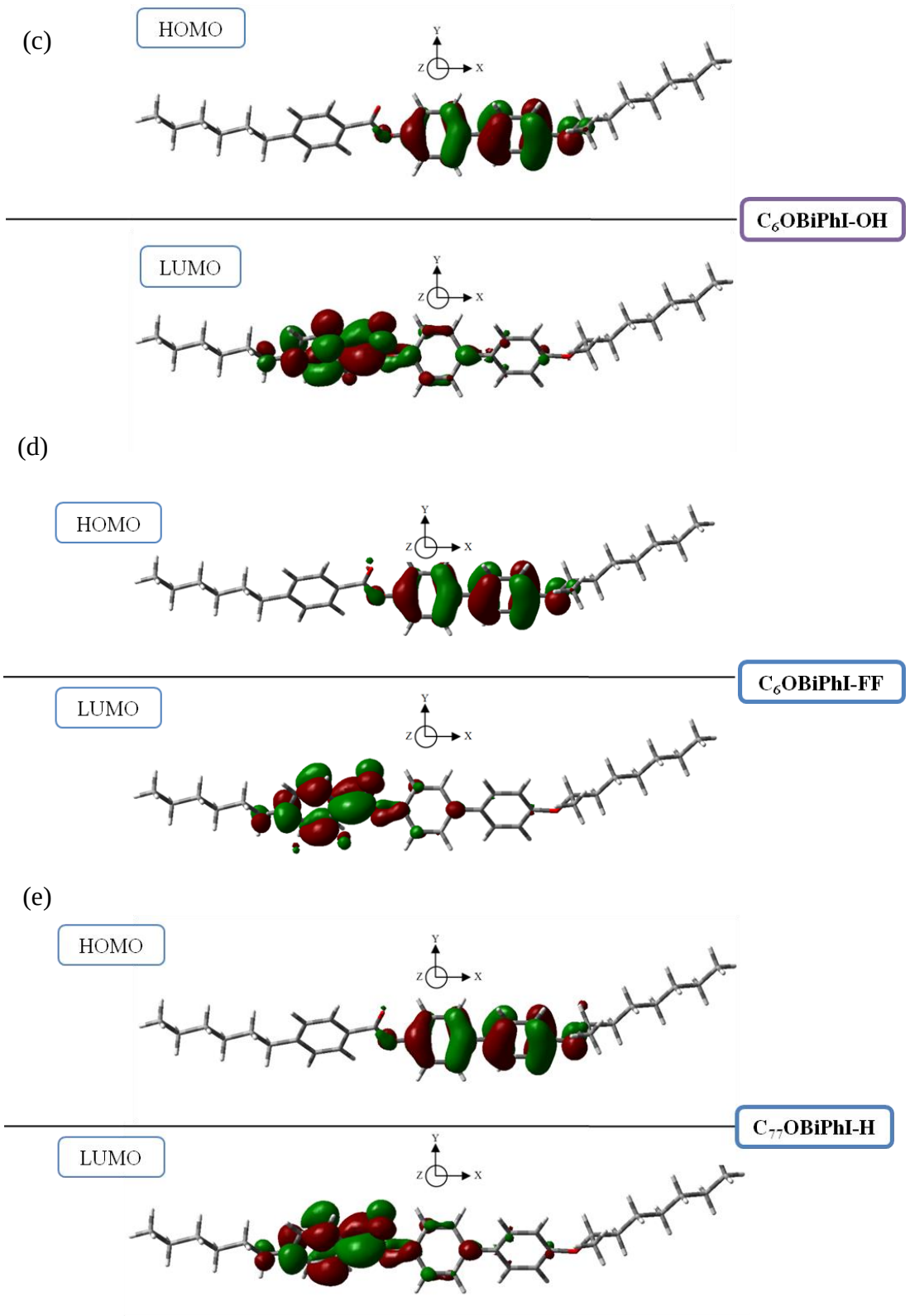

Fig. S19 The HOMO and LUMO of compound (a) **C_6OBiPhI-H** (b) **C_6OBiPhI-F** (c) **C_6OBiPhI-OH** (d) **C_6OBiPhI-FF** (e) **C_{77}OBiPhI-H**. The simulation exchange functional and basis set are CAM-B3LYP and 6-311G(d, p), respectively. The isosurface is drawn at value of 0.02

Table S1. DFT calculated HOMO, LUMO, energy gap, dipole moment components, μ_x, μ_y, μ_z and modulus (μ) for the biphenyl compounds.

Compound	Energy (eV)			Dipole moment (m in Debye)			
	HOMO	LUMO	ΔE (eV)	μ_x	μ_y	μ_z	μ_{total}
C_6OBiPhI-H	-7.0074	0.0123	7.0196	-1.4837	0.5665	0.3023	1.6166
C_6OBiPhI-F	-6.9789	-0.1483	6.8306	-2.3668	1.1911	0.9564	2.8170
C_6OBiPhI-OH	-7.1621	-0.0172	7.1449	0.5034	1.2278	1.3010	1.8584
C_6OBiPhI-FF	-7.0240	-0.2903	6.7337	-1.7324	2.2723	1.6355	3.2923
C_{77}OBiPhI-H	-7.0492	0.0023	7.0515	-1.5766	0.4402	0.2524	1.6562